Chen et al., http://www.jcb.org/cgi/content/full/jcb.201507035/DC1

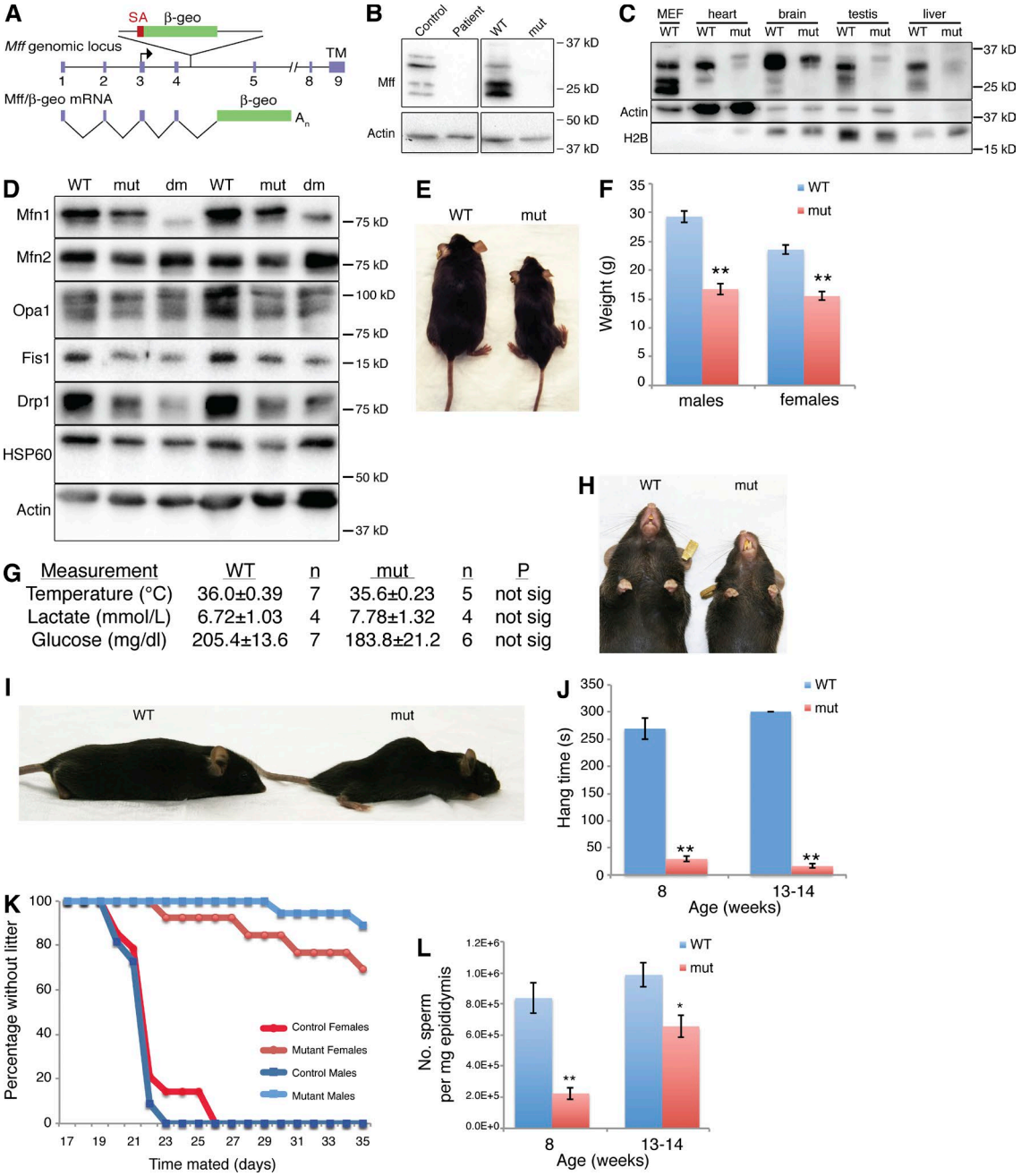

Figure S1. **Pleiotropic phenotypes in *Mff*^{gt} mice.** (A) Schematic depicting gene trap insert in *Mff* locus and subsequently truncated mRNA. The exon/intron structure is derived from Ensembl (transcript ID: ENSMUST00000078332). Exon 3 is the first coding exon, and exon 9 encodes the transmembrane (TM) segment. Based on DNA sequence analysis, the gene trap vector pGT01xr with splice acceptor (SA) and lacZ/neomycin phosophotransferase fusion gene (β-geo) is inserted immediately after the sequence 5′-GCACTCCTCTGTCTGCCTTG-3′ in the intron following exon 4. Exon 4 is equivalent to exon 2 of human *Mff*, as depicted in Fig. 2 in the original *Mff* report (Gandre-Babbe and van der Bliek, 2008). Human exon 2 and mouse exon 4 encode the R1 and R2 motifs essential for Drp1 recruitment (Otera et al., 2010). Human exon 2 is present in all human *Mff* splice isoforms (Gandre-Babbe and van der Bliek, 2008), and mouse exon 4 is present in all four mouse isoforms predicted in UniProt. As a result, the gene trap insertion is ideally positioned to disrupt all Mff isoforms. (B) Western blot analysis of cells with *Mff* mutations. The left panel shows lysates from control and patient fibroblasts containing the truncating mutation Q64X (Shamseldin et al., 2012). The patient fibroblasts show loss of all isoforms. The right panel shows lysates from wild-type and *Mff*^{gt} MEFs. The *Mff*^{gt} MEFs show loss of all isoforms. (C) Western blot showing loss of Mff protein in *Mff*^{gt} tissues. Actin and histone 2B were used as loading controls. (D) Western blot analysis of mitochondrial dynamics proteins in heart lysates. HSP60 was used as a loading control for mitochondrial protein, and actin was used for cytoplasmic protein. (E and F) Decreased size of mutant mice ($n \geq 9$). (G) Measurements of various physiological parameters. (H) Malocclusion. (I) Kyphosis. (J) Hang time from rack while inverted ($n \geq 6$). (K) Decreased fertility of *Mff* mutants. Days without a litter after placement into mating cage were counted ($n \geq 11$). (L) Reduced sperm count of *Mff*^{gt} males ($n \geq 10$). Error bars = SEM. *, $P \leq 0.01$; **, $P \leq 0.001$. WT, wild type.

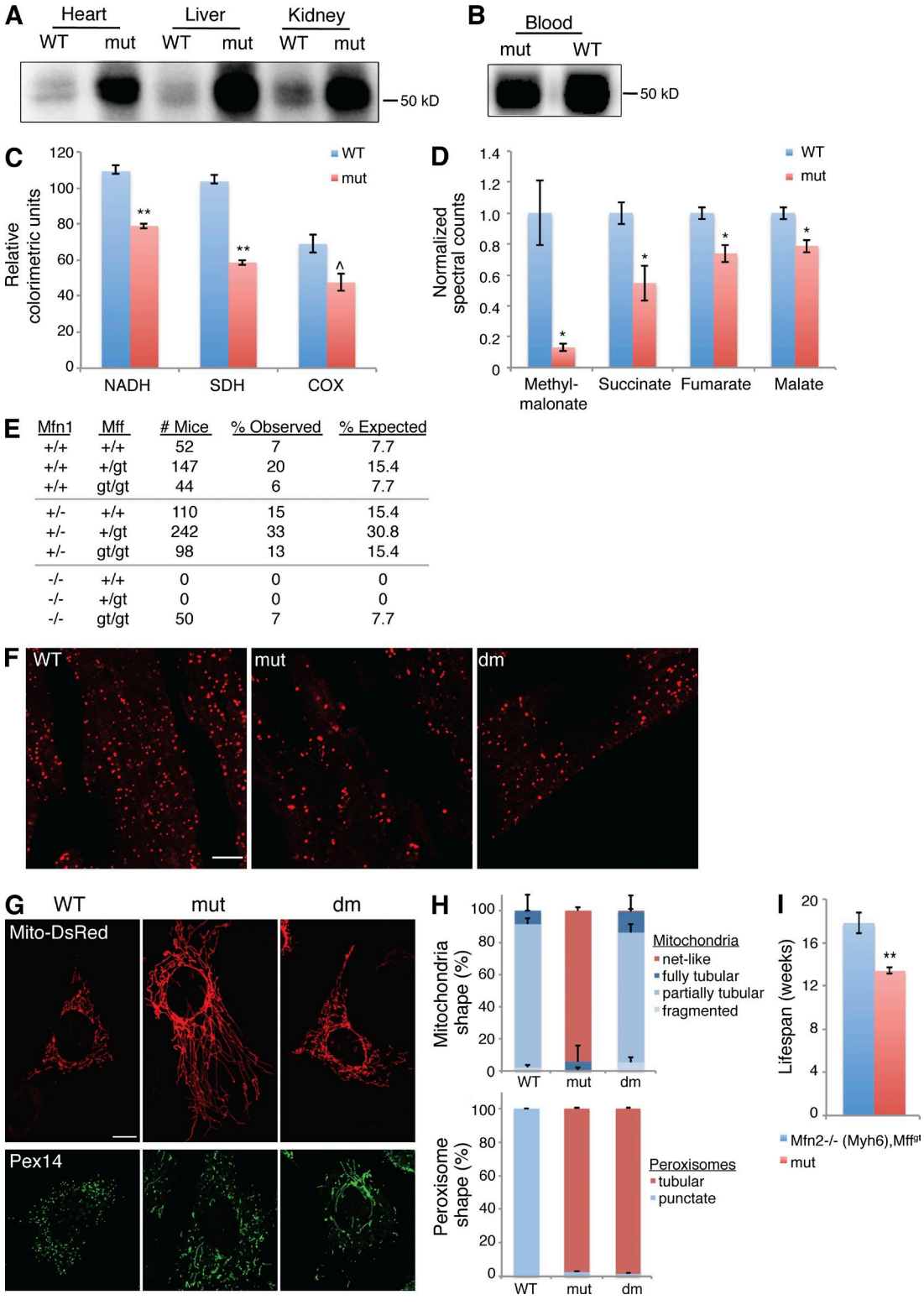

Mfn1	Mff	# Mice	% Observed	% Expected
+/+	+/+	52	7	7.7
+/+	+/gt	147	20	15.4
+/+	gt/gt	44	6	7.7
+/-	+/+	110	15	15.4
+/-	+/gt	242	33	30.8
+/-	gt/gt	98	13	15.4
-/-	+/+	0	0	0
-/-	+/gt	0	0	0
-/-	gt/gt	50	7	7.7

Figure S2. **Additional phenotypes and genetic interaction of Mff with mitofusins.** (A) Western blot of IgG levels in the indicated tissues. (B) IgG levels in blood. (C) Quantification of histochemical staining of respiration complexes in heart ($n = 6$). (D) Metabolomics of Krebs cycle intermediates in heart. Mutants have decreased levels of citric acid cycle components and methylmalonate, which is readily converted to succinyl-CoA ($n = 5$). (E) Weanling numbers from *Mff*$^{gt/+}$,*Mfn1*$^{loxP/loxP}$ × *Mff*$^{gt/+}$,*Mfn1*$^{+/-}$,*Sox2-Cre* cross used to generate *dm* mice. The fifth column lists the expected frequencies if the genotype *Mfn1*$^{-/-}$ is lethal except when combined with *Mff*^{gt} (gt). *Sox2-Cre* drives *loxP* recombination in the epiblast (Hayashi et al., 2002) to generate a whole-body deletion of *Mfn1*. (F) Pex14 stain of peroxisomes in heart. No obvious differences in morphology were found. (G and H) Mitochondrial and peroxisomal morphology in MEFs. *Mff* mutants have elongated mitochondria (mito-DsRed) and peroxisomes (Pex14). Mitochondrial shape is restored in *dm* cells, but peroxisomes remain elongated. (I) Life span of *Mff* mutant mice with and without *Mfn2* deletion in the heart ($n \geq 5$). Error bars = SEM. ^, $P \leq 0.05$; *, $P \leq 0.01$; **, $P \leq 0.001$. Bars, 10 µm.

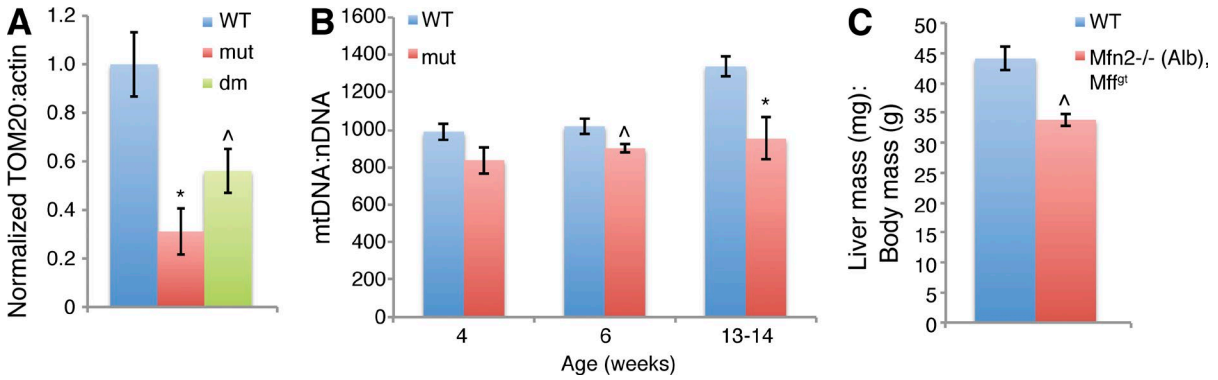

Figure S3. **Loss of mitochondrial protein, mtDNA, and liver mass in *Mff*^{gt} mice.** (A) Ratio of TOM20 (mitochondrial) to actin (cytoplasmic) protein levels in heart. (B) Longitudinal quantification of mtDNA levels in hearts. The mtDNA level is normalized to nuclear DNA (nDNA). A greater discrepancy exists in older animals as mtDNA content increases in wild-type mice but remains constant in mutants ($n \geq 6$). (C) Liver mass adjusted to body size. Deletion of *Mfn2* by *Alb-Cre* does not prevent the size decrease seen in *Mff*^{gt} livers ($n = 2$). Error bars = SEM. ^, $P \leq 0.05$; *, $P \leq 0.01$.

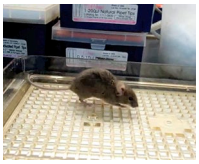

Video 1. **Mff gait alterations.** As the 13-wk-old *Mff* mutant walks, it wobbles from side to side and takes higher steps than is typical of wild-type mice, while holding its tail close to the ground. A wild-type littermate illustrates the difference in gait; it moves more smoothly and rapidly and tends to hold its tail up. Video was acquired at 30 frames per second with a digital video camera recorder (DCR-HC48; Sony).

References

Gandre-Babbe, S., and A.M. van der Bliek. 2008. The novel tail-anchored membrane protein Mff controls mitochondrial and peroxisomal fission in mammalian cells. *Mol. Biol. Cell.* 19:2402–2412. http://dx.doi.org/10.1091/mbc.E07-12-1287

Hayashi, S., P. Lewis, L. Pevny, and A.P. McMahon. 2002. Efficient gene modulation in mouse epiblast using a *Sox2Cre* transgenic mouse strain. *Mech. Dev.* 119:S97–S101. http://dx.doi.org/10.1016/S0925-4773(03)00099-6

Otera, H., C. Wang, M.M. Cleland, K. Setoguchi, S. Yokota, R.J. Youle, and K. Mihara. 2010. Mff is an essential factor for mitochondrial recruitment of Drp1 during mitochondrial fission in mammalian cells. *J. Cell Biol.* 191:1141–1158. http://dx.doi.org/10.1083/jcb.201007152

Shamseldin, H.E., M. Alshammari, T. Al-Sheddi, M.A. Salih, H. Alkhalidi, A. Kentab, G.M. Repetto, M. Hashem, and F.S. Alkuraya. 2012. Genomic analysis of mitochondrial diseases in a consanguineous population reveals novel candidate disease genes. *J. Med. Genet.* 49:234–241. http://dx.doi.org/10.1136/jmedgenet-2012-100836